

Infrared Interferometric Observations of Young Stellar Objects ¹

R.L. Akeson^{2,3}, D.R. Ciardi⁴, G.T. van Belle³, M.J. Creech-Eakman³ and E.A. Lada⁴

ABSTRACT

We present infrared observations of four young stellar objects using the Palomar Testbed Interferometer (PTI). For three of the sources, T Tau, MWC 147 and SU Aur, the 2.2 μm emission is resolved at PTI's nominal fringe spacing of 4 milliarcsec (mas), while the emission region of AB Aur is over-resolved on this scale. We fit the observations with simple circumstellar material distributions and compare our data to the predictions of accretion disk models inferred from spectral energy distributions. We find that the infrared emission region is tenths of AU in size for T Tau and SU Aur and ~ 1 AU for MWC 147.

Subject headings: stars:pre-main sequence, circumstellar matter

1. Introduction

Observational evidence for circumstellar material around most young stellar objects (YSOs) includes infrared emission in excess of that expected from the stellar photosphere, broad forbidden line profiles, and emission at millimeter wavelengths. Although the dust column density is inferred to be quite high, the sources are often optically visible, implying a geometrically flat distribution of the material. A disk morphology is also predicted by star formation theories as a consequence of conservation of angular momentum. Evidence for circumstellar disks has been observed around sources with a range of masses, from near solar (T Tauri stars) to greater than 10 M_{\odot} (Herbig Ae/Be stars) (see e.g. Mundy, Looney and Welch (2000); Natta, Grinin and Mannings (2000)). Disks not only provide a conduit for material to accrete onto the central star, but are also a reservoir of material from which a potential planetary system might form.

The structure of YSO circumstellar disks has been studied using spectral energy distributions (SED), spectral line profiles and imaging at infrared and (sub)-millimeter wavelengths. The dust continuum emission from disks around several T Tauri sources has been resolved at millimeter wavelengths (see review by Wilner and Lay (2000)). These observations are sensitive to emission

¹to be published in the *Astrophysical Journal*

²Infrared Processing and Analysis Center, California Institute of Technology MS 100-22, Pasadena, CA, 91125

³Jet Propulsion Laboratory, MS 171-113, 4800 Oak Grove, Pasadena, CA 91109

⁴University of Florida, 211 Bryant Space Sciences Bldg, Gainesville, FL 32611

from cooler dust and provide spatial information on size scales of several 10's of AU. The disk physical properties on much smaller scales ($< \text{few AU}$) are generally inferred through examination of the spectral line shapes and modeling of the SED. Unresolved issues regarding the inner disk structure include the possible existence of inner disk holes (e.g. Hillenbrand et al. (1992)) and the validity of simple power law scalings to describe globally the temperature and density profiles of the disk. Characterizing the physical properties of the inner disk is important for theories of hydrodynamic disk winds and for understanding the initial conditions of planet formation.

Infrared interferometry provides a method to directly observe the inner disk. To date, only a few YSOs have been observed using this technique (e.g. FU Ori: Malbet et al. (1998) and AB Aur: Millan-Gabet et al. (1999)). Here we present K-band long baseline interferometric observations of four YSOs: T Tau, SU Aur, AB Aur, and MWC 147. PTI has a fringe spacing of ~ 4 mas, corresponding to 0.6 AU at the distance of Taurus-Aurigae (140 pc) and to 3 AU at the distance of MWC 147 (800 pc).

2. Observations and data reduction

Observations were made in the K band at PTI, which is described by Colavita et al. (1999). The data were obtained between September and December 1999. For each source, the number of nights, the total number of records (each of which contains 25 seconds of data) and the calibrators used are given in Table 1. The data were calibrated using the standard method described in Boden et al. (1998). A synthetic wideband channel is formed from the five spectrometer channels. The system visibility is measured with respect to the calibrators. The calibrator sizes were estimated using a blackbody fit to photometric data from the literature and were confirmed to be internally consistent when two or more calibrators were observed in a given night, which occurred on most nights. The calibrators were chosen by their proximity to the sources and for their small angular size, minimizing systematic errors in deriving the system visibility. All calibrators used in this reduction have angular diameters < 0.8 mas and were assigned uncertainties of 0.1 mas, except for HD 46709 ($\theta = 1.8 \pm 0.2$ mas). The data are presented in normalized squared visibility, which is an unbiased quantity. The averaged squared visibility and error are given for each source in Table 1. The uncertainties for the calibrated visibilities are a combination of the calibrator size uncertainty and the internal scatter in the data.

3. Models

Of the four objects discussed in this paper, three were resolved and the fourth was over-resolved (no fringes were detected). In this section we first detail the models and then discuss each source separately in the following section. The models fit to the data are a uniform brightness profile, a Gaussian brightness profile, and a binary companion. We also compare the data to accretion disk

models. The uniform and Gaussian profiles are presented as simple geometric distributions which can be used as size scale estimators. At the distances to these systems (140 to 800 pc) the central star is unresolved ($\theta < 0.1$ mas). For the uniform and Gaussian distributions and the accretion disk models, a stellar component has been included as an unresolved source with the appropriate flux ratio. This ratio was determined by subtracting the photospheric flux from a star of the appropriate spectral type from the total K band flux. For these objects, the infrared emission on milliarcsec scales is dominated by thermal emission and scattering can be neglected (Malbet and Bertout 1995).

3.1. Uniform and Gaussian profiles

Two of the simplest geometric models which can be used to describe the circumstellar material distribution are a uniform brightness profile and a Gaussian profile. For a face-on Gaussian or uniform profile, the predicted visibility is simply a function of the projected baseline. For the uniform profile, the squared visibility is

$$V^2 = \left[\frac{2J_1(\pi\theta B_p/\lambda)}{\pi\theta B_p/\lambda} \right]^2 \quad (1)$$

where J_1 is a Bessel function, θ is the diameter, and B_p is the projected baseline. For a Gaussian profile

$$V^2 = \left(\exp \left[-\frac{\pi^2}{\ln 2} \left(\frac{D}{2} \right)^2 \frac{B_p^2}{\lambda} \right] \right)^2 \quad (2)$$

where D is the FWHM.

For an inclined profile, the visibility is also a function of hour angle. As none of the sources show definitive visibility structure with hour angle, we limit ourselves to the simple face-on case. The observations cover hour angle ranges of -2 to 2 hours for T Tau, -2 to 0 hours for SU Aur and -3 to 1 hours for MWC 147. Although other inclinations and position angles are not necessarily excluded by the data, we note that inclination angles near edge-on would produce significant visibility variations with hour angle, which are not seen. The best fit uniform and Gaussian profile sizes for each source are given in Table 1.

3.2. Binary companion

A reduction from unity visibility can be produced by a binary companion. If both components are individually unresolved, the visibility is given by

$$V^2 = \frac{1 + R^2 + 2R \cos[(2\pi/\lambda)\mathbf{B} \cdot \mathbf{s}]}{(1 + R)^2} \quad (3)$$

where R is the flux ratio, \mathbf{B} is the baseline vector and \mathbf{s} (in radians) is the binary angular separation vector. To test if the measured visibilities are consistent with a binary, a grid of binary parameters was formed and model visibilities were calculated and compared to data binned by projected baseline. The binary parameter space considered contained primary/secondary flux ratios (R) from 1 to 30 and separations (s) up to 100 mas, which corresponds to the coherence length of the spectral channels. Binary companions beyond this separation with sufficient magnitude to affect the measured visibility have been ruled out by speckle or adaptive optics observations (T Tau and SU Aur, Ghez et al. (1993); MWC147, Cororon (1998)).

3.3. Accretion disk

Emission from an accretion disk is one of the leading explanations for the infrared excess and other observed features of T Tauri stars and has also been proposed for Herbig Ae/Be stars. One common method of describing the physical properties of the accretion disk is to parameterize the temperature (T) and surface density (Σ) as power-law functions of the radius ($T \propto r^{-q}, \Sigma \propto r^{-p}$) and the dust opacity as a power-law function of wavelength ($\kappa \propto \lambda^\alpha$). At $2.2 \mu\text{m}$ the disk is optically thick and the emission profile at a given radius depends on the temperature distribution (Beckwith et al. 1990). As we have only sampled one spatial scale in the disk, we will use accretion disk models from the literature, where the SED or millimeter imaging has been used to determine the disk parameters.

4. Results

4.1. T Tau

T Tauri, one of the best-studied YSOs, has an infrared companion, T Tau S, $0''.7$ to the south, which is optically obscured. Both components have a near-infrared excess, suggestive of circumstellar material. Recent observations (Koresko 2000) have revealed that T Tau S is also a binary. The millimeter wave flux is dominated by material surrounding T Tau N and is consistent with circumstellar disk models with an outer radius of 40 AU (Akeson et al. 1998).

At K band, T Tau N is the component with higher flux and thus, it contributes most to the measured visibility. The binary separation is sufficiently large such that the fringe envelopes of the two sources do not overlap and thus T Tau S does not contribute any coherent flux. However, it is within the field of view of the star and fringe trackers and therefore contributes incoherent flux, reducing the observed V^2 on T Tau N by $R^2/(1+R)^2$, where R is the flux ratio between T Tau N and S. For these observations the ratio has two components, the intrinsic K band flux ratio of the system and an instrumental flux ratio introduced by an optical fiber, both of which are discussed below.

At PTI, the angle tracking passband is 0.7-1.0 μm . T Tau N is brighter than T Tau S in the visible, Stapelfeldt et al. (1998) measured a ratio of >2000 in the I band; thus the field will be centered on T Tau N. As the optical path for the spectrometer channels includes a fiber with 1'' FWHM, the flux contribution from T Tau S is reduced. The relative coupling of the N/S flux was calculated in the following way. An Airy pattern given by the diffraction limit of $1''.2$ was convolved with a 1'' Gaussian representing the seeing. We then use a matched filter of a Gaussian with 1'' FWHM for the fiber, which is centered on T Tau N. The errors were conservatively estimated by assuming the fiber FWHM to have an error of 50%. The resulting fiber coupling ratio (N/S) is 1.50 ± 0.2 .

The total flux and flux ratio for the T Tau system varies on time scales of weeks to months (e.g. Skrutskie et al. (1996)) and so roughly contemporaneous flux ratios are necessary. T. Beck (private communication) measured a N-S flux ratio of 1.96 ± 0.19 on 31 Oct 1999. The last four nights of our data were taken on 20 and 26 Oct and 2 and 3 Nov 1999. In the analysis below, we assume the flux ratio measured by Beck is valid for these 4 nights and use only these data.

We note that we have no direct way of knowing that the detected fringes arise from T Tau N instead of T Tau S. An alternate explanation for the detection is that the fringes arise from T Tau S. If this were the case, the expected visibility with T Tau S unresolved is $V^2=0.07$, much lower than that observed. The low visibility is due to the flux and fiber ratios still favoring T Tau N and would be even lower if T Tau S were resolved. The stability of the fringe tracking and the consistency of the night to night measurements strongly suggest that only 1 of the binary components is detected, and given the above argument, we deduce that T Tau N is the detected component.

To correct for T Tau S, the visibilities were divided by $R^2/(1 + R)^2$ before modeling was performed, where R represents the correction for both the intrinsic flux ratio and the coupling effect described above and is 2.94 ± 0.48 . For the stellar parameters estimated by Ghez et al. (1991) using optical photometry, the total to stellar flux ratio at K is 3.6 for T Tau N. The stellar contribution is included in the models as an unresolved component. The visibilities show a slight dependence on hour angle, but more data are needed to confirm this effect.

The data were reduced and binned by projected baseline before being fit by Gaussian and uniform profile models. The best fit uniform profile diameter is $2.62_{-0.044}^{+0.046}$ mas (0.37 AU) and the best fit Gaussian has a FWHM of $1.61_{-0.031}^{+0.028}$ mas (0.22 AU) (Figure 1a). For the accretion disk model, we have used the parameters derived by Ghez et al. (1991) with $r_{inner} = 0.04$ AU, $r_{outer} = 100$ AU, a temperature profile $T \propto r^{-0.42}$ and $T(1 \text{ AU}) = 260$ K. This accretion disk model overestimates the measured visibility and, thus, underestimates the size scale. Using the disk parameters derived by Akeson et al. (1998) from millimeter wave emission ($r_{inner} = 0.01$ AU, $r_{outer} = 40$ AU, $T \propto r^{-0.6}$, $T(1 \text{ AU}) = 100$ K), the predicted size is even smaller than the Ghez model.

The binary parameters which fit the measured visibilities are shown in Figure 1b, where the

contours are for χ_r^2 of 1, 2 and 4. We note that if a binary companion at the separation shown in Figure 1b were in a roughly circular orbit around T Tau N, we should have seen visibility changes in the data given the time span covered by the observations. However, no time dependence was seen in the data.

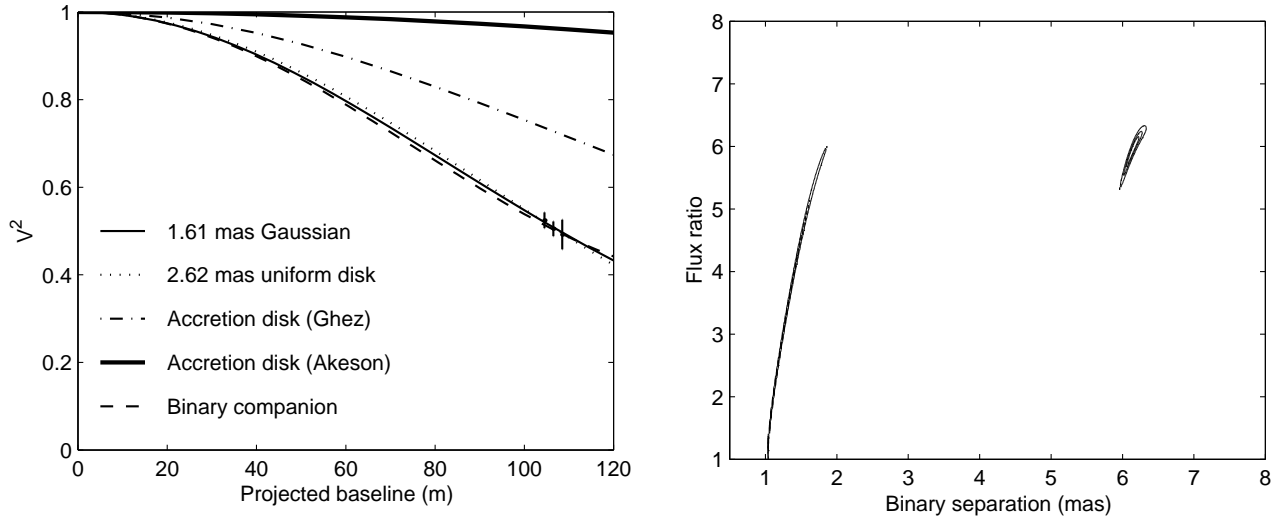


Fig. 1.— Binned data and models for T Tau. The models are Gaussian profile (solid line), uniform profile (dotted line), accretion disk from Ghez et al. (1991) (dash-dot line), accretion disk from Akeson et al. (1998) (thick solid line at top) and binary companion (dashed line). The plotted visibilities have been corrected for the incoherent flux of T Tau S, as described in §4.1. The binary parameters represented are separation of 1.5 mas and a flux ratio of 4.3. b) Contour plot of possible binary companion parameters. The contour levels represent models with a χ_r^2 of 1, 2, and 4.

4.2. SU Aur

SU Aur is a T Tauri star with an SED similar to that of T Tau. Herbig and Bell (1988) designated SU Aur as the prototype of a separate classification from weak-line T Tauris due to its broad absorption lines and high luminosity ($\sim 12 L_\odot$). The stellar/total flux ratio at K is 0.3 (Marsh and Mahoney 1992). The best fit diameters are $1.92^{+0.063}_{-0.059}$ mas and $1.16^{+0.038}_{-0.039}$ mas for a uniform profile and a Gaussian (FWHM) respectively (Figure 2a). This corresponds to a physical size of 0.27 and 0.16 AU for a distance of 140 pc. The accretion disk model is taken from Beckwith et al. (1990) with $r_{inner} = 0.01$ AU, $r_{outer} = 100$ AU, a temperature profile $T \propto r^{-0.51}$ and $T(1 \text{ AU}) = 260$ K, where the parameters were determined by fitting $10 \mu\text{m}$ through millimeter wave fluxes. This model underestimates the observed visibility.

The binary parameter space for models with reduced chi-squared, χ_r^2 of 1, 2 and 4 is shown

in Figure 2b. The pattern shown in the figure repeats in separation space to roughly 20 mas. The binary companion hypothesis for SU Aur is not well constrained due to the limited time and baseline coverage of the data. The time coverage we do have favors orbiting companions with separations at roughly 2 or 6 mas.

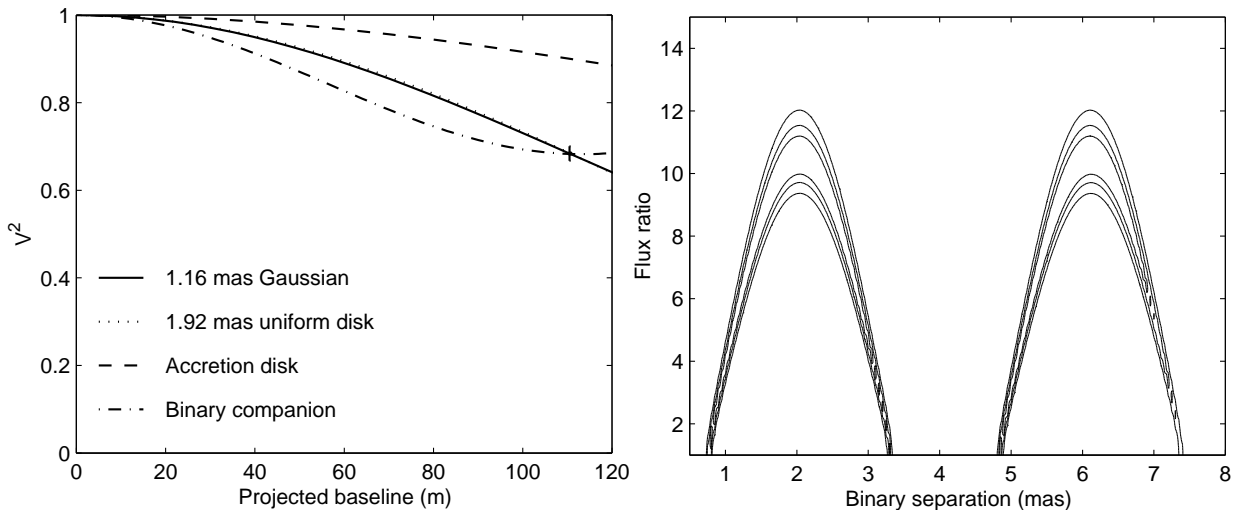


Fig. 2.— a) Binned data and models for SU Aur. The models are Gaussian profile (solid line), uniform profile (dotted line), accretion disk (dashed line) and binary companion (dash-dot line). The binary parameters represented are separation of 2 mas and a flux ratio of 10. b) Contour plot of possible binary companion parameters. Note that this pattern repeats in separation space to 20 mas. The contour levels represent models with a χ_r^2 of 1, 2, and 4.

4.3. MWC 147

MWC 147 (HD 259431) is a Herbig Ae/Be star with spectral classifications in the literature ranging from B2 to B6. Hillenbrand et al. (1992) modeled the SED from this source as arising from a flat, optically thick disk with an inner hole. Previous studies have used a distance to this source of 800 pc, which we will use here for consistency, although we note a recent distance determination from Hipparcos data of 290_{-84}^{+200} pc (Bertout et al. 1999). If the distance to MWC 147 is ~ 290 pc, the physical sizes given below decrease by a factor of 2.8. Depending upon which spectral type is used, the stellar contribution to the flux at K is 0.05 to 0.1 of the total. We use an unresolved component with 0.1 of the total flux to represent the central star in these models. Using a stellar contribution of 0.05 would increase the squared visibility due to the disk by 4%.

The data were reduced as described above and binned by projected baseline. The data and models are shown in Figure 3a. Given the errors on the individual data points, there is no significant

dependence on hour angle in the visibility data, consistent with Millan-Gabet (1999b). The best fit uniform profile diameter is $2.28^{+0.017}_{-0.034}$ mas (1.8 AU) and the best fit Gaussian has a FWHM of $1.38^{+0.013}_{-0.014}$ mas (1.1 AU). The accretion disk and stellar parameters were taken from Hillenbrand et al. (1992) with $r_{inner} = 0.36$ AU, $r_{outer} = 1.8$ AU and a temperature profile $T \propto r^{-3/4}$. The reference temperature is set by the stellar temperature, 2×10^4 K, and the accretion rate, $\dot{M} = 10^{-5} M_{\odot}/\text{year}$. As seen in Figure 3a, this accretion disk model underestimates the measured visibility and so overestimates the physical size.

The observed visibilities for MWC 147 can also be explained by a binary companion. Figure 3b shows the parameter space for binary models with reduced χ_r^2 of 1, 2, and 4. An adaptive optics survey by Corporon (1998) found a binary companion to MWC 147 with a separation of $3''.1$ and magnitude difference $\Delta K = 5.7$. This source is too widely separated and too faint to have affected our observations.

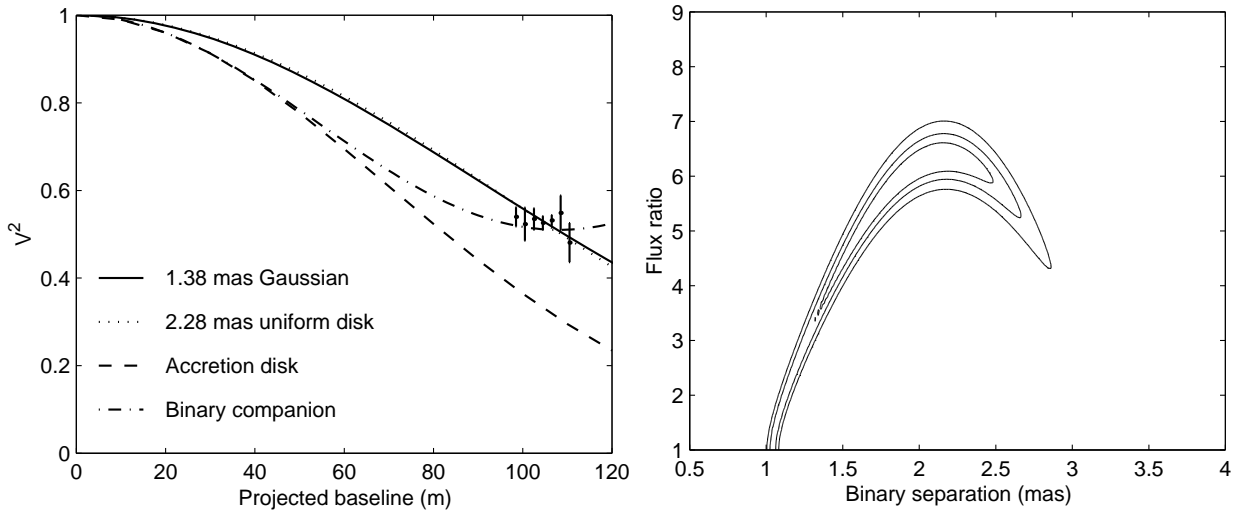


Fig. 3.— a) Binned data and models for MWC 147. The models are Gaussian disk (solid line), uniform disk (dotted line), accretion disk (dashed line) and binary companion (dash-dot line). The binary parameters represented are a separation of 2.1 mas and a flux ratio of 6. b) Contour plot of possible binary companion parameters. The contour levels represent models with a χ_r^2 of 1, 2, and 4.

4.4. AB Aur

AB Aur is a Herbig Ae/Be star with a spectral type of A0, at a distance of 140 pc. Millan-Gabet et al. (1999) resolved the infrared emission from this source with the IOTA interferometer using baselines of 21 and 38 m. At PTI, fringes were not detected on AB Aur, despite a photon

flux higher than that for T Tau, indicating that the AB Aur is too large to be detected on baselines of ~ 100 m with current sensitivities. Upper limits were found for the visibility using the sensitivity of the detection algorithm and measuring the system visibility with a calibrator. At K band, the estimated upper limit was $\langle V^2 \rangle < 0.08 \pm 0.02$, which corresponds to a size $> 4.1(\pm 0.2)$ mas (0.57 AU) diameter for a uniform profile and $> 2.7(\pm 0.1)$ mas (0.38 AU) for a Gaussian. These results are consistent with the size and derived by Millan-Gabet et al. (1999) and a previous upper limit from PTI of $\langle V^2 \rangle < 0.3$ from Berger (1998).

5. Discussion

The fundamental result of these observations is that for all four sources observed here, the infrared emission arising from circumstellar material is resolved by PTI with a nominal fringe spacing of 4 mas. The measured sizes correspond to physical scales of tenths of AU for the T Tauri sources T Tau and SU Aur and ~ 1 AU for the Herbig Ae/Be star MWC 147. We note that if the correct distance for MWC 147 is 290 pc, rather than 800 pc, then the measured visibility corresponds to a size scale of roughly 0.5 AU, similar to that measured for the T Tauri sources, despite the large difference in stellar mass. Our measured visibilities do not agree with those predicted from accretion disk models derived from near-infrared SEDs or millimeter interferometric observations. This may suggest that the single power-law relations used to describe the temperature and density are inadequate to reproduce both the spectral and spatial characteristics of the emission.

Our data on T Tau and SU Aur require the K band emission to come from a larger region than that predicted by the accretion disk models, while the opposite is true for MWC 147. Millan-Gabet (1999b) observed 15 Herbig Ae/Bes using infrared interferometry with a shorter baseline and found that roughly half of the sources could not be well modeled as emission from an accretion disk and that the predicted visibilities were higher than the observed data. On the other hand, Malbet et al. (1998) used PTI for observations of FU Ori and found that an accretion disk model could explain the measured visibilities.

Further characterization of the circumstellar material on size scales less than one AU can be achieved by extending the infrared interferometry observations presented here. PTI has a second baseline, which provides data on shorter spacings, and is equipped to observe in the H band, which probes higher temperatures and has higher spatial resolution than K band. We plan to extend our study of young stellar objects to include H band and more spatial scales.

This work was performed at the Infrared Processing and Analysis Center, Caltech and the Jet Propulsion Laboratory. Data were obtained at the Palomar Observatory using the NASA Palomar Testbed Interferometer, which is supported by NASA contracts to the Jet Propulsion Laboratory. Science operations with PTI are possible through the efforts of the PTI Collaboration (<http://huey.jpl.nasa.gov/palomar/ptimembers.html>). We particularly thank A. Boden for

his efforts in data reduction software and B. Thompson for useful discussions. We are also grateful to T. Beck for providing the T Tau flux ratio. DRC acknowledges support from NASA WIRE ADP NAG5-6751. EAL acknowledges support from a Research Corporation Innovation Award and a Presidential Early Career Award for Scientists and Engineers to the University of Florida.

REFERENCES

- Akeson, R. L., Koerner, D. W., and Jensen, E. L. N. 1998, *ApJ*, 505, 358
- Beckwith, S. V. W., Sargent, A. I., Chini, R. S., and Gusten, R. 1990, *AJ*, 99, 924
- Berger, J.P. 1998, Ph.D. thesis, Univ. Joseph Fourier de Grenoble, France
- Bertout, C., Robichon, N., and Arenou, F. 1999, *A&A*, 352, 574
- Boden, A. F., Colavita, M. M., van Belle, G. T., and Shao, M. 1998, *SPIE proceedings*, 3350, 872
- Colavita M. M. et al 1999, *ApJ*, 510, 505
- Corporon, P. 1998, Ph.D. thesis, Univ. Joseph Fourier de Grenoble, France
- Ghez, A. M., Neugebauer, G., Gorham, P. W., Haniff, C. A., Kulkarni, S. R., Matthews, K., Koresko, C., and Beckwith, S. 1991, *AJ*, 102, 2066
- Ghez, A. M., Neugebauer, G., and Matthews, K. 1993, *AJ*, 106, 2005
- Herbig, G.H. and Bell, K.R. 1988, *Lick Obs. Bull.* 111, Third Catalog of Emission-line Stars for the Orion Population (Santa Cruz: Univ. California)
- Hillenbrand, L. A., Strom, S. E., Vrba, F. J., and Keene, J. 1992, *ApJ*, 397, 613
- Koresko, C.D., 2000, *ApJ*, 531, 147
- Malbet, F., et al 1998, *ApJ*, 507, 149
- Malbet, F. and Bertout, C. 1995, *A&AS*, 113, 369
- Marsh, K. A. and Mahoney, M. J. 1992 *ApJ*, 395, 115
- Millan-Gabet, R., Schloerb, F. P., Traub, W. A., Malbet, F., Berger, J. P., and Bregman, J. D. 1999, *ApJ*, 513, 131
- Millan-Gabet, R. 1999, Ph.D. thesis, University of Massachusetts
- Mundy, L.G., Looney, L.W. and Welch, W.J. 2000, in *Protostars and Planet IV*, ed. V. Mannings, A.P. Boss and S.S. Russell (Tucson: University of Arizona), in press

Natta, A., Grinin, V.P., and Mannings, V. 2000, in Protostars and Planet IV, ed. V. Mannings, A.P. Boss and S.S. Russell (Tucson: University of Arizona), in press

Skrutskie, M. F., Meyer, M. R., Whalen, D. & Hamilton, C. 1996, AJ, 112, 2168

Stapelfeldt, K. R. et al. 1998, ApJ, 508, 736

Wilner, D.J. and Lay, O.P. 2000, in Protostars and Planets IV, ed. V. Mannings, A.P. Boss and S.S. Russell (Tucson: University of Arizona Press), in press

This preprint was prepared with the AAS L^AT_EX macros v5.0.

Table 1. PTI observations

Source	# of nights (records)	Calibrators	$\langle V^2 \rangle$	Uniform disk ^a (diameter)	Gaussian ^a (FWHM)
T Tau	4(119)	HD 28024, HD 27946	0.29 ± 0.01^b	$2.62^{+0.046}_{-0.044}$ mas	$1.61^{+0.028}_{-0.031}$ mas
SU Aur	3(38)	HD 28024, HD 27946, HD 25867	0.68 ± 0.02	$1.92^{+0.063}_{-0.059}$ mas	$1.16^{+0.038}_{-0.039}$ mas
MWC 147	9(121)	HD 43042, HD 46709	0.53 ± 0.01	$2.28^{+0.017}_{-0.034}$ mas	$1.38^{+0.013}_{-0.014}$ mas
AB Aur	4 ^c	HD 32301	< 0.15	> 3.7 mas	> 2.4 mas

^a1 σ uncertainties are given for the best fit Gaussian and uniform disk models.

^bThe visibility given for T Tau is the calibrated value uncorrected for the effects of T Tau S.

^cOnly nights with good upper limits are listed for AB Aur